Journal of Indian Geomorphology
Volume 13, 2025 ● ISSN 2320-0731
Indian Institute of Geomorphologists (IGI)

Geospatial Approach to Assess the Erosion Susceptibility by Morphometry and RUSLE in the Mayurakshi Drainage Basin, Eastern India

Subha Roy[1], Souvik Das[1], Jaya Chatterjee[1], Md. Hasanur Jaman[1], Prakash Mistri[2] and Somasis Sengupta[1]

[1]*Department of Geography, The University of Burdwan, Bardhaman - 713104*

[2]*Department of Geography, Kishore Bharati Bhagini Nivedita College, Kolkata - 700060*

E-mail: ssengupta@geo.buruniv.ac.in *(Corresponding author)*

Abstract: *The article attempts to predict the amount of soil loss occurring in the Mayurakshi Basin, with the help of morphometry based and the empirical model Revised Universal Soil Loss Equation RUSLE). The Analytical Hierarchy Process (AHP) was carried out for ascertaining the erosion susceptibility of the area under consideration by morphometric attributes. The methodology followed essentially differs from the traditional AHP technique because while assigning weights to multiple parameters, the traditional AHP technique takes into consideration the opinion of the experts. Hence, the study has depended on the Principal Component Analysis (PCA) before assigning weights to the conditioning morphometric parameters for pairwise comparison in AHP. The actual soil loss occurring in the studied basin was estimated with the help of the RUSLE. The erosion hotspots were identified with the help of Z-Scores (Z>3). Using the Receiver Operating Characteristic (ROC) Curve, the reliability and interrelationship of the two models was estimated. The Area Under the Curve (AUC) is about 0.739. This implies that the reliability of the two models is about 73.90%, which is reasonably acceptable. Here, the Sensitivity (Sn) is 51.00% and Specificity (Sp) is 78.60%, which means that Sp>Sn. This indicates that both the models are comparable.*

Keywords: Erosion; morphometry; Analytical Hierarchy Process; Receiver Operating Characteristic Curve; sensitivity; specificity.

Introduction

The complex interplay between topography, lithology, climate and tectonics at different spatio-temporal scales represents (Mesa, 2006; Angillieri, 2008; Evans, 2012) one of the most regarded fundamental geomorphic units — the drainage basin (Gregory, 1999). Encompassing the entire region which provides runoff to the trunk stream and its tributaries, the shape and morphology of the basin controls various geomorphic and hydrologic processes operating within it. Understanding the prevailing morphology, geomorphic and hydrologic processes operating within a basin is required for quantitative analysis.

Morphometric attributes collectively refer to the quantitative attributes, are the numeric parameters that are derived from the terrain or elevation surface and drainage network within a catchment (Goudie, 2004). Since 2000, Digital Elevation Models (DEMs) have found a place in different aspects of geomorphology viz. terrain erosion susceptibility (Kadam *et al.,* 2019; Asfaw and Workineh, 2019; Prabhakar *et al.,* 2019), flash flood hazard (Mesa, 2006; Angillieri, 2008; Bhat *et al.,* 2019), watershed hydrological regime (Sreedevi *et al.,* 2013; Rawat and Mishra, 2016; Bezinska and Stoyanov, 2019) and tectonic control and litho-structure (Kuhni and Pfiffner, 2001; Kale *et al.,* 2014).

More or less, physical factors, (drainage basin morphometry) beside the land cover and anthropogenic activities greatly affect erosion. In the domain of integrated watershed management, the assessment and estimation of the erosion status of a watershed is often the prerequisite. However, its exact quantification, especially along the major tributaries, is difficult and often not feasible, particularly for a basin which is larger in areal extent (Singh *et al.,* 2008). Drainage basin morphometry determines the spatial pattern of erosion susceptibility in a drainage basin. This process is mainly index based employing multiple parameters weighted in accordance with their relative importance. AHP is one of the most popular multi-criteria models used in the field of earth science for assessing erosion susceptibility (Kachouri *et al.,* 2014; Haidara *et al.,* 2019; Das *et al.,* 2015 and the references therein)

Number of factors affect the process of soil erosion, operating in tandem (Wischmeier and Smith, 1978; Renard *et al.,* 1997; Mutua *et al.,* 2006; Butt *et al.,* 2010). Surface runoff is one of the most important driving factors of soil erosion, other environmental and physiographic parameters such as, precipitation, soil characteristics and slope, in affected in the global context (Civeira *et al.,* 2016a, 2016b; Dutta *et al.,* 2017; Oliveira *et al.,* 2019). Land use modification, deforestation, construction activities and agricultural practices are those anthropogenic factors which have been playing a role in soil loss and degradation. Land use land cover pattern is one of the most significant factors affecting the amount of soil loss in a catchment or any other areal unit. Characteristic of soil and surface runoff correspondingly changes with frequent alteration in land use (Setegn *et al.,* 2010; Gebremicael *et al.,* 2013; Kim *et al.,* 2013). In many developing countries of the world, population is governed by agricultural activities. Therefore, soil erosion becomes an important quasi-natural hazard and appropriate management of the soil is an important exercise in this domain (Kim *et al.,* 2005; Lim *et al.,* 2005). Predicting the annual rate of soil loss across different basins, spatially varying in areal extent is an important domain in earth sciences with the help of models such as, Universal Soil Loss Equation (USLE) and Revised Universal Soil Loss Equation (RUSLE) (Lee, 2004; Pandey *et al.,* 2009; Kumar and Gupta, 2016). Rainfall erosivity (R), soil erodibility (K), slope length and steepness (LS), crop management (C) and conservation support practice (P) are five major factors to be used in the RUSLE model (Sheikh *et al.,* 2011). These five parameters influencing erosion risk act as proxies for both the physical (slope, precipitation and pedology) and anthropogenic (land use, conservation practices, etc.) (Farhan *et al.,* 2013).

In this study, an attempt has been made to evaluate the soil erosion susceptibility with

the help of MCDM-devised morphometric parameters. Although, several studies are available in literature wherein such morphometry-based erosion potential has been estimated (Sarkar *et al.,* 2021; Roy *et al.,* 2022), one of the fundamental limitations of morphometry-based analysis is that there is no scope of employing other factors such as soil, land use, etc. Since erosion is often associated with such pedologic and anthropogenic factors in addition to the terrain factors, overlooking the former factors may often introduce errors in the results. This may pose a significant hindrance to the micro-level planning for soil erosion. Therefore, this study incorporates the RUSLE-based soil loss estimation and final validation of the morphometry-based erosion susceptibility and the RUSLE-based total soil loss in the Mayurakshi basin This is significant because similar to the previous studies on morphometry, studies on RUSLE are usually in isolation (Panagos *et al.,* 2017, Das *et al.,* 2018). There has been a dearth of significant attempts to correlate and validate the two. Therefore, the primary objective of the study is to estimate erosion susceptibility and annual soil loss by morphometry-based MCDM and RUSLE, respectively. Secondly, the study aims to validate the two models and assess their reliability. Finally, this study aims to identify the erosion hotspots wherein significant soil conservation strategies can be employed.

Study area

The Mayurakshi basin of eastern India has been selected as areal unit of the study in this analysis (Fig. 1). The entire region is enclosed between 24°29′ N to 23º54′ N and 86°49′ E to 88°12′ E, thereby encompassing an area of roughly 9,596 km2 (Islam and Deb Barman, 2020). This basin can be divided into three major sub-basins namely the Kopai, the Dwarka and the Brahmani, the Mayurakshi being the largest among them. The Mayurakshi river originates from the Trikut hill of the Chotanagpur plateau, about 16 km from the Deoghar town in the state of Jharkhand in eastern India. The Mayurakshi river flows to the east. The river traverses a course of about 250 km, extending across the Indian states of Jharkhand (Deoghar and Dumka districts) and West Bengal (Birbhum and Murshidabad districts and some part of Purba Bardhaman). The Kopai river, with a length of 137 km, originates at Jalalpur (23°45′43″ N, 87°23′10″ E) and meets the Mayurakshi at Talgram (23°51′45″ N, 88°2′33″ E).

The Dwarka river (154 km long) originates near Gopikander in the Santhal Pargana Division in Jharkhand at an elevation of 141 m ASL (24°27′6’’ N, 87°27′23″ E). This river gets the waters of the Brahmani river, which is 120 km in length, at Hazipur (24°9′23″ N, 88°0′21″ E).

The annual soil loss of the Mayurakshi drainage basin has been calculated using the Morphometry parameters based on MCDM model and Revised Universal Soil Loss Equation (RUSLE) (Fig. 2) as postulated by Renard et al. (1997).

Calculation of morphometric parameters

The calculation of morphometric parameters of the Mayurakshi drainage basin was essentially based on the DEM. The Advanced Land Observing Satellite Phased Array L-Band Synthetic Aperture Radar (ALOS-PALSAR) DEM data was used as the input dataset for morphometric analysis. This 12.5 m resolution ortho-DEM (Scene 1: ALPSRP055230540, Path–505, Frame–540, Scene–2: ALPSRP055230530, Path–505, Frame–530) was downloaded from the

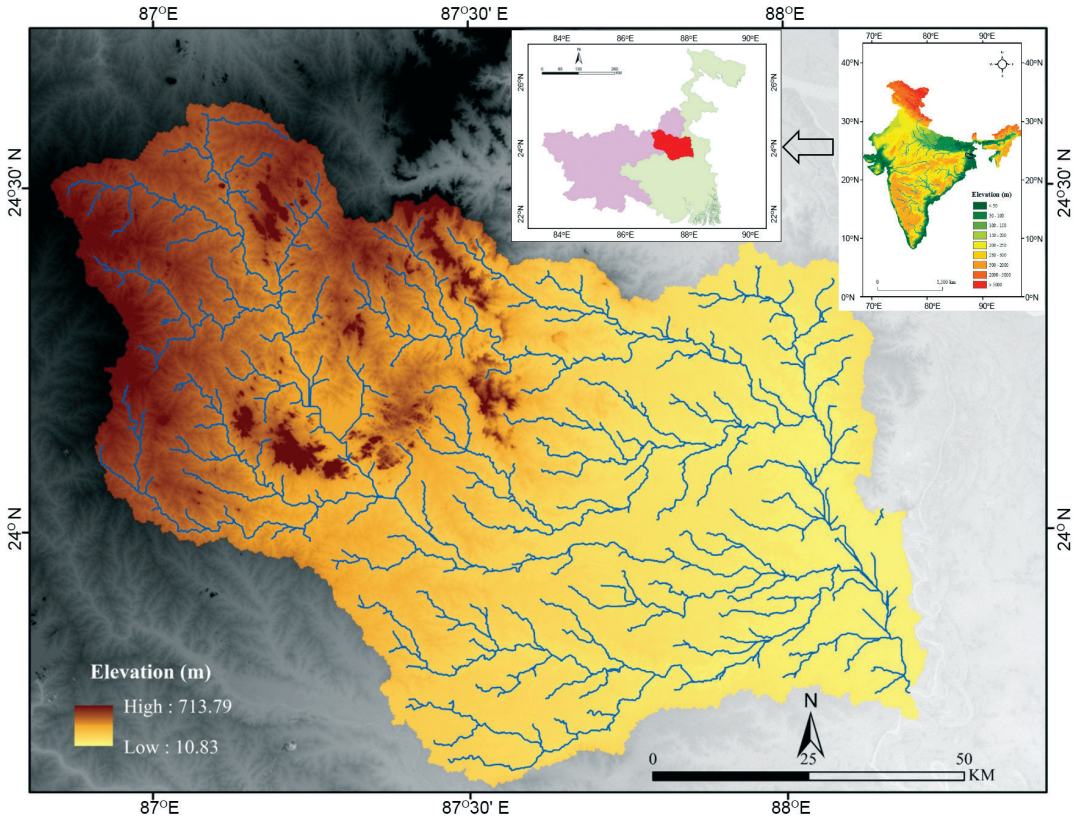

Figure 1. DEM of the Mayurakshi river Basin showing the drainage network. Inset: DEM of India and location of the Mayurakshi Basin within the Indian states of West Bengal and Jharkhand

Alaska Satellite Facility Distributed Active Archive Centre (https://www.earthdata.nasa.gov/centers/asf-daac). The DEM was preferred over other freely available DEMs because of its higher resolution which helps in better delineation of drainage networks and watersheds (Niipele and Chen, 2019; Sarkar *et al.,* 2021; Roy *et al.,* 2022). Since this DEM provides ellipsoidal heights, it is unsuitable for further processing in its raw form. Therefore, the Earth's Gravity Model (EGM 2008) was employed to correct the dataset, as recommended by Pavlis et al. (2012). Then the DEM was imported into an ArcGIS environment, and the possible data gaps were filled. Then the D8 method was employed in ArcGIS for assigning the flow directions. This method, which assigns the flow routes based on the maximum direction of descent, is the most popular flow direction algorithm in DEM literature. Next, the drainage accumulation metric was created by employing the 'Flow Accumulation' command in ArcGIS. This accumulation metric was processed in ArcGIS after a threshold was decided for drainage identification. After testing multiple threshold values, a threshold of 100 pixels was selected, as the resulting drainage network most closely matched the Survey of India topographical maps at 1:50,000 scale. Subsequently, the 'Watershed' tool in ArcGIS was used to delineate the Mayurakshi watershed.

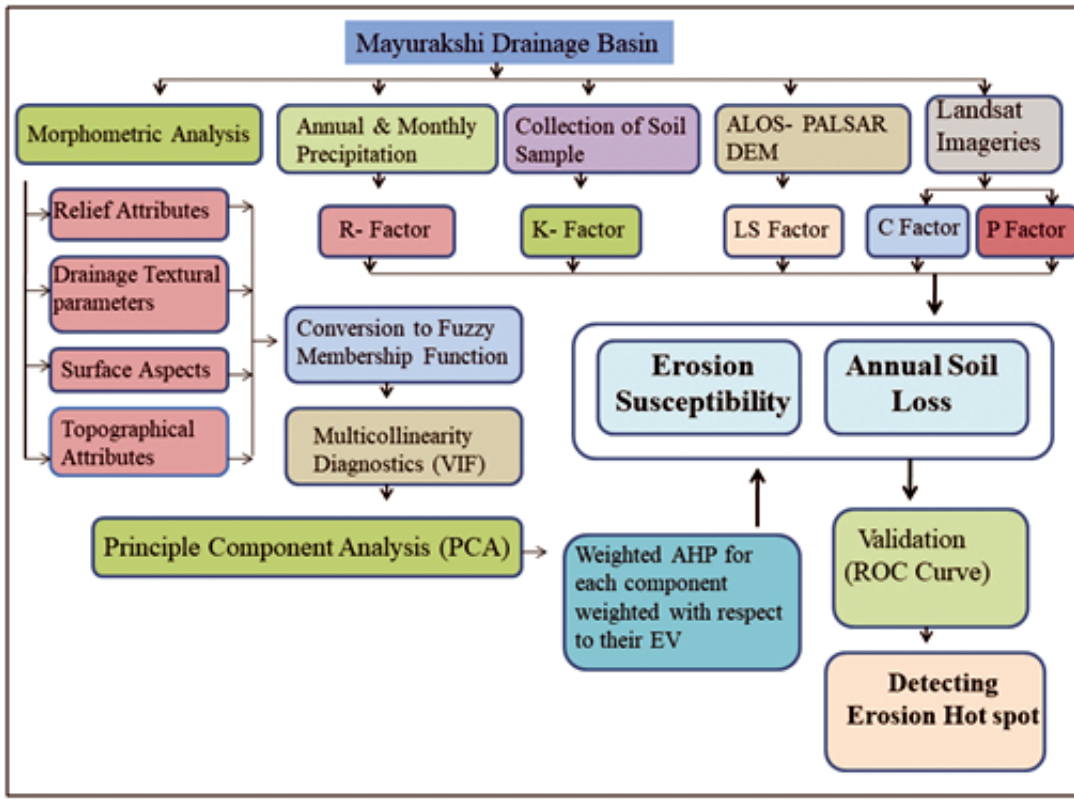

Figure 2. The flow chart of methodology

Table 1. Formula of all morphometric parameters to applied in this study

Sl. No.	Morphometric Parameter	Formula	Variables	Reference
01	Relative Relief (Rr)	$Rr = H_{max}-H_{min}$	H_{max} = Maximum Elevation and H_{min} = Minimum Elevation	Strahler (1956)
02	Dissection Index (DI)	$DI = Rr/ H_{max}$	Rr = Relative Relief and H_{max} = Maximum Elevation	Nir (1957)
03	Hypsometric Integral (HI)	$HI = (H_{mean}-H_{min})/ (H_{max}-H_{min})$	H_{nean} = Mean elevation of the basin, H_{min} = Minimum elevation of the basin and H_{max} = Maximum elevation of the basin	Pike and Wilson (1971)
04	Slope(θ)	1st derivative of DEM surface		Evans (1980)
05	Curvature	2nd derivative of DEM surface		Evans (1980)
06	Drainage density (D_d)	$D_d = L_u / W_a$	L_u = Total length of all the streams in the basin, W_a = Basin area	Horton (1945)
07	Stream frequency (S_f)	$S_f = N_u / W_a$	N_u = Total number of all streams, W_a = Basin area	Horton (1945)

Sl. No.	Morphometric Parameter	Formula	Variables	Reference
08	Constant of Channel Maintenance (CCM)	$CCM = 1/D_d$	D_d = Drainage Density	Schumm (1956)
09	Length of Overland Flow (LOF)	$LOF = 1/D_d \times 2$	D_d = Drainage Density	Horton (1945)
10	Ruggedness Number (R_n)	$R_n = (Rr \times D_d) / 1000$	Rr = Relative Relief, D_d = Drainage Density	Melton (1965)
11	Topographic Wetness Index (TWI)	$TWI = \ln [A_s / \tan(\theta)]$	A_s = Specific Catchment Area derived from the accumulation matrix, θ = Slope in radians	Moore and Burch (1986a)
12	Stream Power Index (SPI)	$SPI = \ln [A_s \times \tan (\theta)]$	A_s = Specific Catchment Area derived from the accumulation matrix, θ = Slope in radians	Moore *et al.* (1991)

After the identification of the Mayurakshi river's drainage network and watershed, various morphometric parameters were calculated in ArcGIS 10.5 platform. Such parameters viz., drainage density, dissection index, curvature, hypsometric integral, relative relief, slope, stream power index, topographic wetness index, length of overland flow, stream frequency, constant of channel maintenance, ruggedness number and infiltration number were calculated from the standard formulae postulated by previous workers (Table 1). It is pertinent to mention that ArcGIS has an inherent problem of drainage number ambiguity wherein any linear feature between two nodes is regarded as lines. By the inherent design of ArcGIS, any river after receiving a tributary, gets an additional node. Therefore, it is expected that the number of streams may be amplified erroneously as the same river (line) may have several pairs of nodes. For example, if a river meets three tributaries, three nodes are erroneously generated and hence the count of the river becomes four. Therefore, stream frequency, which counts the number of streams per unit area, may get erroneously amplified. This error was removed by manual verification of each river and all such false nodes were deleted by "Merge" option in the editor toolbar. Therefore, it is expected that the drainage textural parameters generated from the ALOS-PALSAR DEM are reasonably free from the errors associated with the vector data topology.

Normalisation and fuzzification of the parameters

It is pertinent to mention here that different parameter data range and units are different, therefore, he respective parameters were normalised by fuzzification. The MS large fuzzification function was carried out for those parameters which act as positive factors of soil erosion and MS small fuzzification function considered the negative factors for fuzzification (Luo and Dimitrakopoulous 2003) (Eq.1 and 2).

$$f(x)= \begin{cases} 1 - \dfrac{bs}{x - am + bs}, & x > am \\ 0, & \text{otherwise} \end{cases} \quad \text{Eq. 1}$$

where, f(x) is the fuzzy membership function of the attribute x, m = arithmetic mean of the attribute x, s = standard deviation of attribute x, a = mean multiplier (taken as 1) and b = standard deviation multiplier (taken as 1). This function is monotonically increasing which implies that as the value of x increases,

f(x) also increases and vice versa.

$$f(x)=\begin{cases} \dfrac{bs}{x-am+bs}, & x > am \\ 0, & \text{otherwise} \end{cases} \quad \text{Eq. 2}$$

The notations in Eq.2 are the same as that of Eq.1. Unlike the MS large function, the MS small function is monotonically decreasing i.e. with an increase in the value of x, the magnitude of f(x) decreases and vice versa. Therefore, all the rasters of absolute values of individual parameters were converted to fuzzified rasters in ArcGIS.

Multicollinearity diagnostics

Multicollinearity diagnostics was performed to check all morphometric attributes obtained for the Mayurakshi basin. When two or more predictor variables in the dataset are highly correlated, this condition refers to as multicollinearity (Keat *et al.,* 2009; Daoud 2012; Vommi 2017). Redundant variables are introduced in multicollinearity and may often result into introduction of bias in the results (Eq. 3) (Mela and Kopalle 2002). Therefore, removal/detection of multicolinearity (Table 2) is often a prerequisite in multi-criteria decision making.

$$VIF_j = \frac{1}{1-R_j^2} \quad \text{Eq. 3}$$

where VIFj is the Variance Inflation Factor of the i^{th} variable against all other predictor variables, Rj is the regression of the j^{th} independent variable on the remaining (k-1) independent variables. Hence, before performing multiple regression VIF was calculated by taking one variable as dependent variable and all other predictor variables as the independent variables. All other variables in this process were reiterated, and those with a Variance Inflation Factor (VIF) greater than 10 were excluded from the MCDM analysis (Hair *et al.,* 1995).

Table 2: VIF outcomes of different parameters

Variable	VIF	Remarks
Curvature	1.44	Included for PCA and AHP
Dissection Index	2.84	
Hypsometric Integral	3.36	
Drainage density	4.00	
Slope	9.01	
Stream frequency	10.00	
Ruggedness Number	21.28	
Stream Power Index	22.22	
Topographic Wetness Index	23.81	
Infiltration Number	55.56	Removed for PCA and AHP
Relative Relief	83.33	
Length of Overland Flow	> 100	
Constant of Channel Maintenance	> 100	

Multi-criteria-based Erosion Susceptibility Assessment

The complexity of the process of erosion ensures that a large number of variables need to be estimated for quantifying the erosion potential to a reasonable degree of accuracy and precision (Dar *et al.,* 2013). Therefore, erosion is a multi-criteria problem that can be summarised in a generic model as follows (Eq. 4):

$$E_s = f(x_1, x_2, \ldots\ldots\ldots xn) \quad \text{Eq. 4}$$

where Es is the erosion susceptibility index and x_1, x_2, ……. xn are the independent parameters that determine erosion susceptibility (Boender *et al.,* 1989).

Therefore, using multiple parameters for the assessment of erosion susceptibility using multi-criteria decision making (MCDM) models appear in this domain. Saaty (1980) introduced the Analytical Hierarchy Process (AHP) in recent years and gradually the model became one of the most popular MCDM techniques in predicting erosion susceptibility

(Arabameri *et al.,* 2018 and the references therein). According to their relative importance AHP includes a pairwise comparison with a non-parametric scaling 1 to 9.

This pairwise comparison is then used for assigning the relative weights to different parameters. Therefore, it is evident that the success of an AHP exercise depends, to a large extent, on the consistency of the pairwise comparison. This is verified with the help of the Consistency Ratio (CR) given in Eq. 5.

$$CR = CI/RI \quad \text{Eq. 5}$$

where, consistency index (CI) is obtained as (λmaxn)/ (n−1), λmax_n is the weight sum derivative of the AHP-based pairwise comparison matrix, n is the number of criteria and the Random Index (RI) is generated for a pairwise comparison matrix taking 'n' criteria.

This paper proposes the application of Principal Component Analysis (PCA) prior to performing Saaty's parameter scaling. In the field of Earth sciences, particularly geomorphology, this approach is highly popular—especially with the widespread use of PCA. Mather and Doornkamp 1970; Magner and Brooks 2008; Singh *et al.,* 2008; Meshram and Sharma 2017; etc.). Therefore, values were extracted of individual parameters from 50 equally spaced points covering the whole basin and PCA was carried out in SPSS software. Table 3 reveals that the explained variance of the 1st Principle Component (PC) is only 28.5 %, and six (6) PCs considered have a cumulative explained variance of 100%. This is in accordance with the view of Wallis (1965) that the explained variance needs to be very high (greater than 95%) while building models by PCA. Therefore, 0.2850 was weighted factor of 1st component based AHP raster for erosion susceptibility and 0.1985 weight was assigned to the second component based AHP raster. This process was continued for all AHP rasters (6 components) of Mayurakshi basin. The final step involved the summing of the 6 component AHP rasters to generate the erosion susceptibility map of the Mayurakshi basin. (Eq. 6)

$$E_s = \sum_{i=1}^{n} EVi * FAHPi \quad \text{Eq. 6}$$

where, Es = Erosion Susceptibility Score of a river basin, EVi = Explained variance of the i^{th} component and FAHPi = Fuzzified Analytical Hierarchy Process raster obtained for the i^{th} component.

Eq.6 can then be expanded for the Mayurakshi Drainage System in the form of Eq.7.

Table 3: Results of the Principal Component Analysis of the individual parameters

Parameters	L_1[a]	E_1[b]	L_2[a]	E_2[b]	L_3[a]	E_3[b]	L_4[a]	E_4[b]	L_5[a]	E_5[b]	L_6[a]	E_6[b]
DI	0.569		0.138		0.566		0.350		0.413		0.209	
HI	0.711		0.284		0.261		0.244		0.230		0.483	
θ	0.649	28.520	0.355	19.850	0.043	16.084	0.329	14.761	0.510	11.589	0.288	9.196
Cv	0.131		0.620		0.681		0.175		0.316		0.071	
Dd	0.643		0.459		0.192		0.210		0.333		0.429	
Sf	0.176		0.609		0.273		0.721		0.025		0.251	

L_k[a] = Loading score on the kth Component E_k[b] = Explained variance (%) for the kth Component. For notations of parameters, refer Table 1

$$Es = [(FAHP1 \times 0.285) + (FAHP2 \times 0.198) + (FAHP3 \times 0.160) + (FAHP4 \times 0.147) + (FAHP5 * 0.115) + (FAHP6 \times 0.091) /6 \quad \text{Eq. 7}$$

Estimating the annual soil loss by RUSLE model:

One of the essential limitations of the process of ascertaining the erosion susceptibility from drainage basin morphometry is that only the topographic and geomorphic attributes are taken into consideration. However, it is a well-known fact that the sub-aerial process of erosion is often affected by climate, land use and pedologic parameters. Therefore, the results obtained from morphometry may often deviate from the real-world scenario. Therefore, the reliability of the morphometry-based erosion susceptibility can only be ascertained if all such parameters are taken into consideration. Then the actual soil loss can be estimated with the help of such parameters. The Revised Universal Soil Loss Equation (RUSLE), is basically one such model which attempts to quantify the annual loss of topsoil from an areal unit based on certain conditioning factors, comprising both physical and anthropogenic ones. This can be expressed as follows (Renard *et al.,* 1997)

$$A = R \times K \times LS \times C \times P \quad \text{Eq. 8}$$

where, A is the average annual soil loss in an areal unit (tons $ha^{-1}yr^{-1}$), R is the average annual rainfall erosivity factor ($Mjmmha^{-1}h^{-1}yr^{-1}$), K is the soil erodibility factor (th $MJ^{-1}mm^{-1}$), LS corresponds to the dimensionless factor associated with slope-length and slope-steepness, respectively, C is the vegetation cover factor and P is the conservation support practice factor.

In this study, the morphometry-based erosion susceptibility in the studied basin was validated and checked for reliability by the estimated annual soil loss by the RUSLE Model. The RUSLE Model considers the conditioning factors viz., rainfall erosivity (R), soil erodibility (K), slope length and steepness (LS), vegetation cover (C) and conservation support practice (P). The conditioning factors of RUSLE were calculated from the standard formulae postulated by previous workers.

Rainfall erosivity factor (R)

The inherent potential of rainfall to cause erosion is not only dependent on the amount of rainfall, but a large number of other factors such as intensity of rainfall, size of the rain drops, etc. (Blanco-Canqui and Lal, 2008). The erosion potentiality in a particular area depends on average storm rainfall (Das *et al.,* 2018). The long-term average R factor is determined by predicting the rainfall energy (E) and the maximum 30 min rainfall intensity (I30). However, the 30-minute rainfall intensity data for most places of the earth is reasonably lacking (Renard and Freimund, 1994; Lee and Heo, 2011). Considering this, Arnoldus (1980) has computed the R Factor of by an empirical formula which takes into account the monthly as well as the annual rainfall in an area. This equation has been given below:

$$R = 1.735 \times 10 [1.5\log_{10} (MFI) – 0.8188] \quad \text{Eq..9}$$

where, MFI = Modified Fournier Index, which is derived by taking the summation of the individual ratios between the average monthly and the average annual rainfall in an area. Although there are some limitations in this equation, the results obtained from this equation reasonably coincided with the rainfall erosivity values of the Global Rainfall Erosivity Database (GloREDa) (Panagos *et al.,* 2017) which has been prepared by interpolation of the rainfall kinetic energy and

intensity data for 247 stations well distributed across India.

Soil erodibility factor (K)

Despite receiving copious rainfall, often a region may not be affected much by erosion. This is because the ease with which the soil particles can be detached is dependent on the soil texture. The K Factor is a function of various pedologic properties which often determine the ease with which the soil particles may be detached (Haile and Fetene, 2012).

For obtaining the soil erodibility (K Factor), a combination of field-based and laboratory-based methods was used. This was done by dividing the Mayurakshi basin into 2×2 km grids. During the field visit, soil samples were collected at the intersection of the grid lines. Textural analysis was performed using the sieving method which helped in the determination of the percentage of sand, silt and clay. For differentiating the silt and clay percentages, the Robinsons's pipette Method was employed in the laboratory. This way the percentage of sand (S), silt (Si) and clay ratio (C) were determined.

The organic Carbon, which is closely correlated with the organic matter content, was obtained by the Walkley and Black Method in the laboratory. The pH was obtained in the field by the help of a pH Meter. This information was then employed to get the K Factor (David, 1988) (Eq. 10).

$$K = (0.043 \times pH) + (0.62 \div OM) + (0.0082 \times S) - (0.0062 \times C) \times Si \quad \text{Eq. 10}$$

where, K = soil erodibility (t $hMJ^{-1}mm^{-1}$), pH is the acidity/alkalinity of the soil, OM is Organic matter (%), S is Sand content (%), Si is silt content (%) C is clay ratio = % Clay/ (% Sand + % silt)

Slope Length and Steepness Factor (LS)

Soil erosion potential is influenced by topography and in the RUSLE model LS (topography) factor becomes an important component to identify soil loss. Product of the factors of slope length (L) and slope steepness (S) define this factor. Horizontal distance from the origin of overland flow to the specified point defined as Slope and the angle of slope is defined as slope steepness (S). Normally, in soil loss slope steepness (S Factor) is more relevant as compared to the slope length (L Factor) (Wischmeier and Smith, 1978; Thomas *et al.,* 2018).

In this model assessing the LS factor also depends on the flow accumulation, flow direction and the topography of the terrain of the catchment area (Wischmeier and Smith, 1978). Wischmeier and Smith (1978) and Moore and Burch (1986b) developed the equation estimation of the LS factor, and this equation was widely used by Griffin et al. (1988), McCool et al. (1989) and Moore and Wilson (1992). Another LS factor equation proposed by Moore and Burch (1986a, b) and this equation was employed in this study and using the 12.5m resolution ALOS-PALSAR DEM in ArcGIS platform (Eq. 11).

$$LS = \left(\frac{AS}{22.13}\right)^{0.6} \times 1.4 \left(\frac{\sin^1 B}{0.0894}\right)^{1.3} \quad \text{Eq. 11.}$$

where, LS = topography factor, As = Flow Accumulation Raster and B = Slope in radians

Crop Management factor (C)

The C Factor is expressed as the ratio of soil loss from the land covered by the crop patterns under specific conditions to the corresponding loss from uncovered areas such as clean-tilled, water body and fallow land (Wischmeier and Smith, 1978; Renard *et al.,* 1997; Kolli, 2021). The Normalised Bare

Soil Index (NBIL) was computed to quantify the denominator of this fraction i.e. the potential soil loss from an uncovered surface. The Landsat 8 (2018, December) OLI data and Landsat ETM+ for 2008 (December) data used estimated C factor (Eq. 12) in this study (Kolli, 2021).

$$C = \frac{NDVI}{NBIL} \quad \text{Eq. 12}$$

where, C is the Crop Management Factor, NDVI = Normalised Differenced Vegetation Index given as $\frac{NIR-RED}{NIR+RED}$, NBIL = Normalised Bare Soil Index given as $\frac{NIR-SWIR}{NIR+SWIR}$. NIR (Near Infra-Red), SWIR (Short Wave Infra-Red) and RED represent the different bands of multi-spectral imagery.

Support Practices (P)

The P factor defined as ratio between upslope and downslope tillage and soil loss within a specific support practice (Wischmeier and Smith, 1978; Renard and Foster, 1983). For obtaining the P Factor, the images were undergone the Supervised Classification by the Arc GIS software. USDA Handbook No.282(1981) assigned the P factor values of different classes of land use (Wischmeier and Smith, 1978; Renard *et al.,* 1997; Thomas *et al.,* 2018). Ranges of the P Value from 0 to 1 and based (Table 4) on the land use type, P values were assigned to each class.

Results

Morphometric parameters and their spatial variation

The spatial variation in the different morphometric parameters reveals that the middle domain of this basin is characterised by higher relative relief values and the lower values of relative relief are encountered in the upper and the lower domains. Similar to the relative relief, other morphometric parameters such as dissection index, slope, drainage density, stream frequency, infiltration number, ruggedness number and stream power index display elevated values in the middle domain and subdued values in the upper and lower domains. The elevated values of such parameters in the middle domain imply higher erosive potential (Goudie, 2004). The average hypsometric integral for the river basin under consideration is about 0.335. This does not indicate intense erosion. In the studied basin, the curvature, by and large, is negative with some areas of positive curvature found in the middle domain. Smaller values of length of over land flow (LOF) denote high runoff promoting high erosion, and vice versa (Horton, 1932). This fact is typically exemplified in the Mayurakshi drainage basin, which displays higher LOF in the upper domain, suggestive of lower erosion. It is evident from the map displaying the spatial variation in TWI that this parameter tends to increase downstream (Fig. 3 and 4).

Table 4: Values of P factor respected land use/ land cover types

Type	Value
Dense vegetation	0.8
Light vegetation	0.8
Built-up area	2.0
Agricultural land	0.5
Waterbody	1.0
Fallow land	0.9

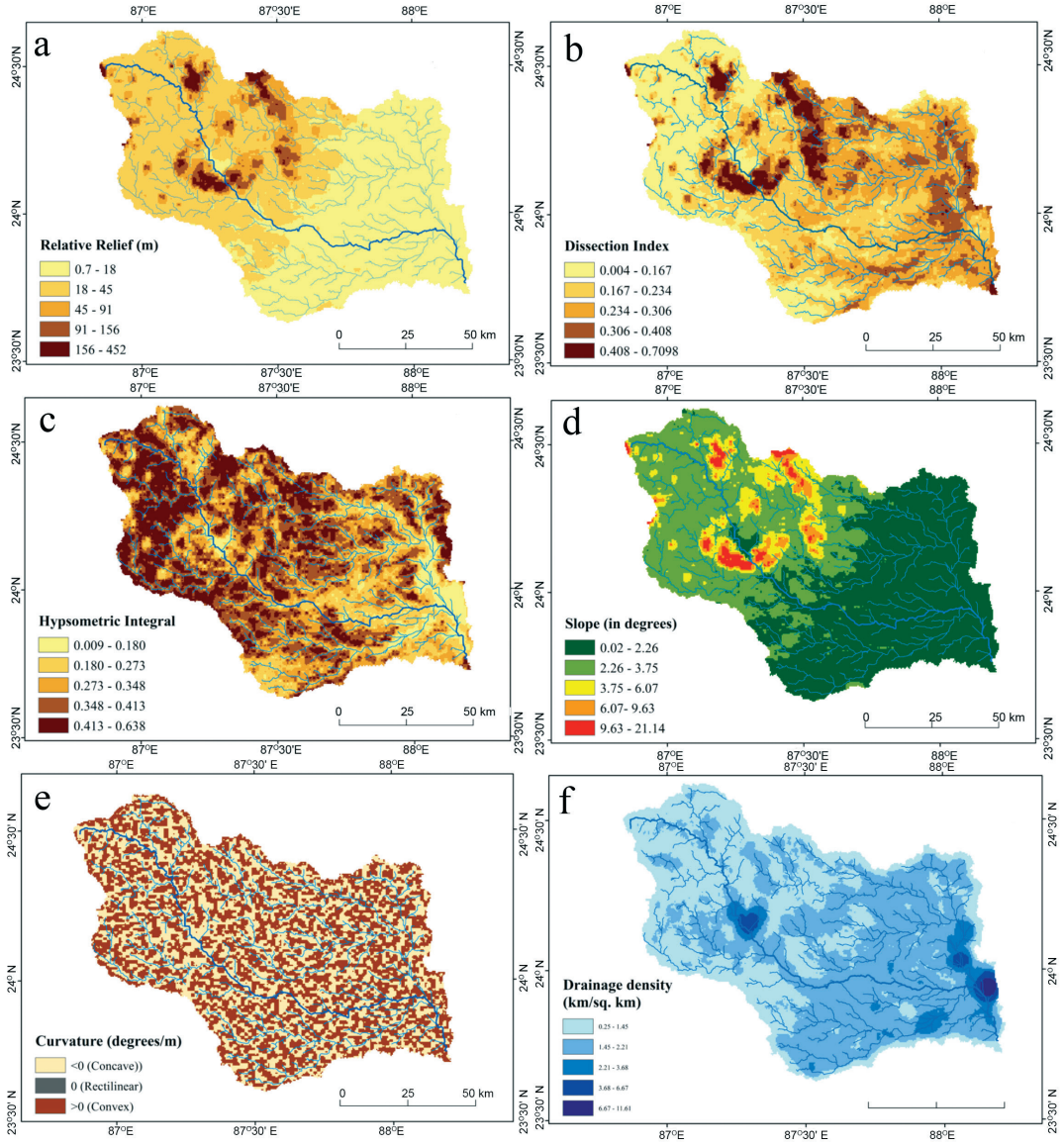

Figure 3. Spatial variation in the morphometric parameters of the Mayurakshi drainage system a) Relative relief b) Dissection Index c) Hypsometric Integral d) Slope e) Curvature f) Drainage density.

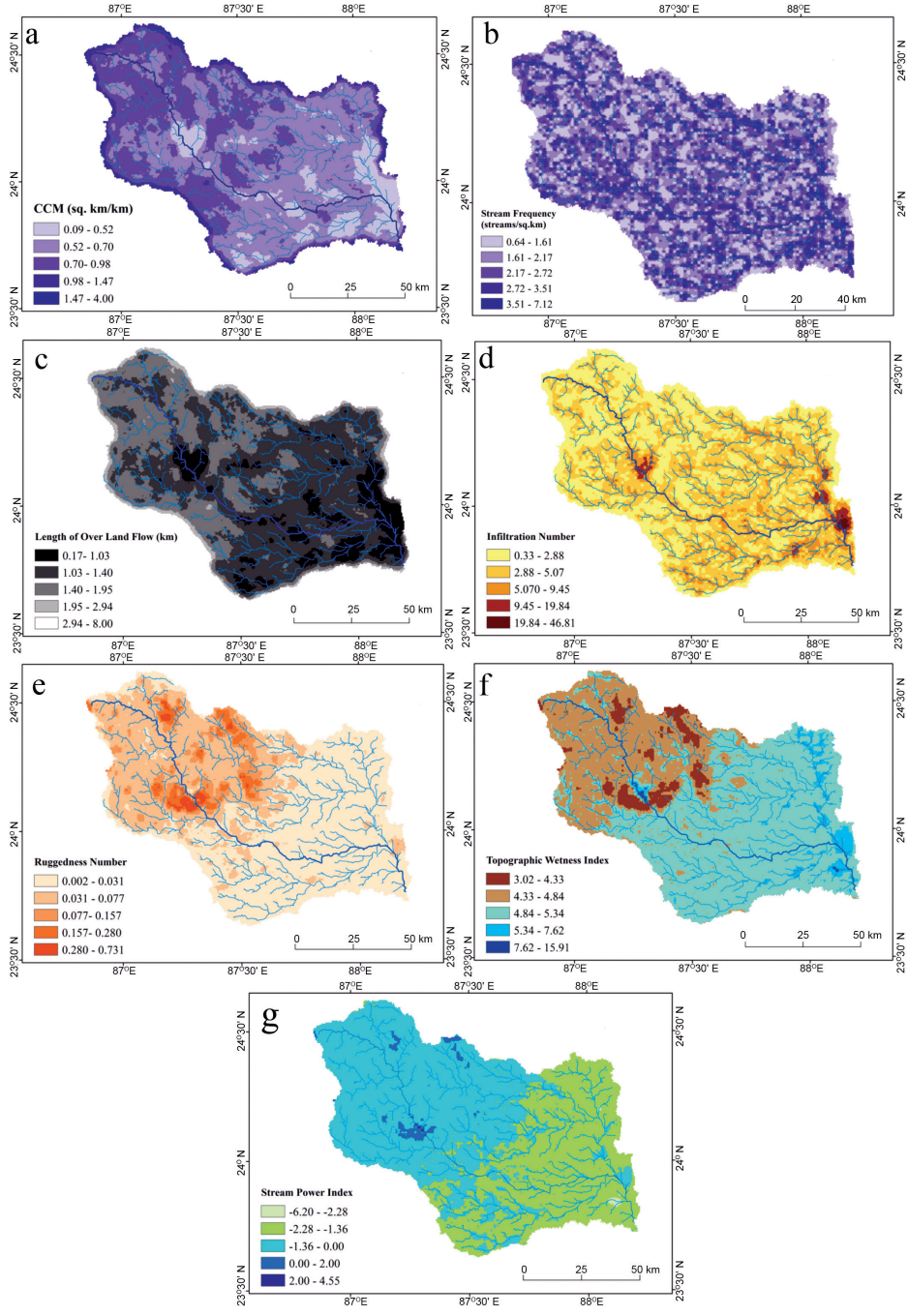

Figure 4. Maps showing the spatial variations in the morphometric parameters a) Constant of Channel Maintenance b) Stream Frequency c) Length of Overland Flow d) Infiltration Number e) Ruggedness Number f) Topographic Wetness Index g) Stream Power Index.

Multicollinearity diagnostics

It has been stated earlier that the Variance Inflation Factor (VIF) was used for ascertaining the multicollinearity of variables. VIF greater than 10 indicate high degree of multicollinearity amongst the predictor variables (Wang *et al.,* 2008; Dormann *et al.,* 2013). The VIF for the ruggedness number, SPI, TWI, infiltration number, relative relief, length of over land flow and constant of

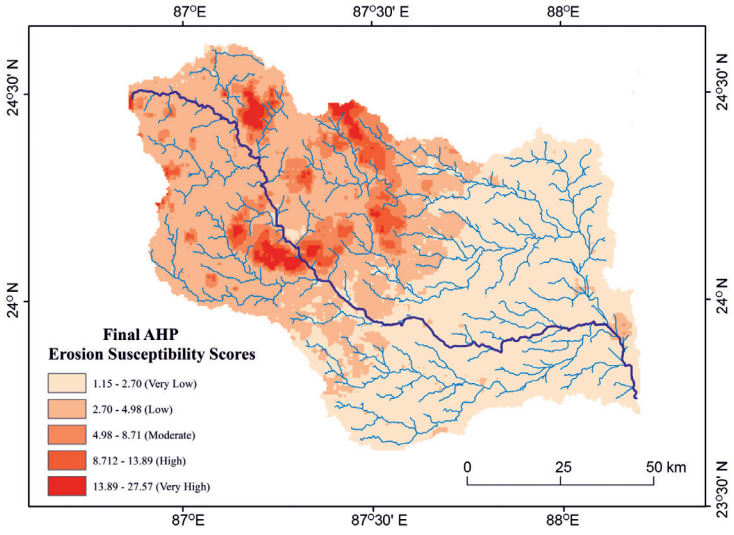

Figure 5: Final Principal Component-weighted AHP-based erosion susceptibility map of Mayurakshi drainage system.

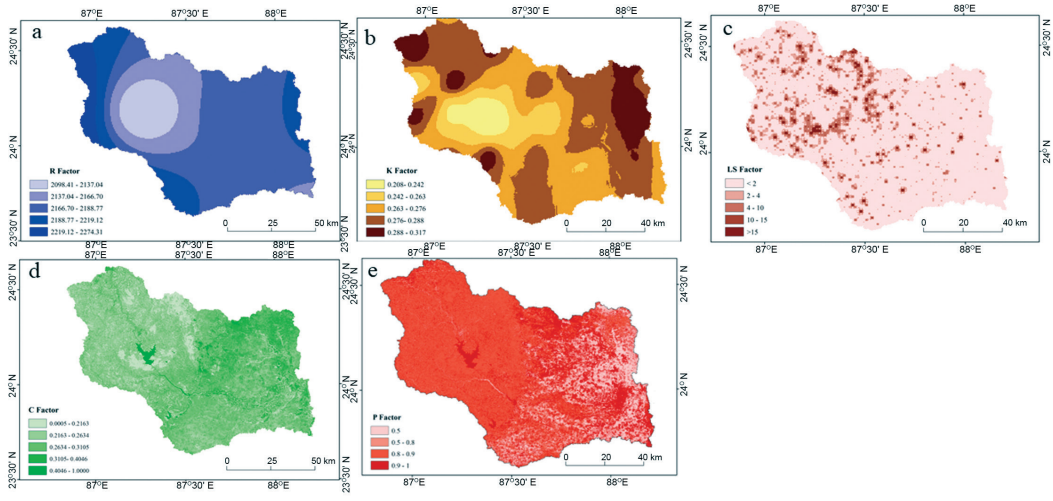

Figure 6. Spatial variation of RUSLE maps the Mayurakshi river basin: a.).R factor, b).soil erodibility factor (K Factor), c).slope length and steepness factor (LS Factor), d).crop management factor (C Factor) and e) support practice factor (P Factor).

channel maintenance are above 10. Therefore, those parameters were removed before the final analysis of erosion susceptibility. Thus, 13 parameters got reduced to 6 parameters which are — curvature, dissection index, hypsometric integral, drainage density, slope and stream frequency.

Multi-criteria Decision Making (MCDM) and erosion potential

Among many MCDM models available to predict erosion susceptibility, the Analytical Hierarchy Process (AHP) is one of the most popular models used in a number of studies in earth sciences (Abdul Rahaman *et al.,* 2015; Das *et al.,* 2020). This model, based on a pairwise comparison matrix (Saaty, 1980) has often been criticised as there is a possibility of ambiguous weight selection (Mistri and Sengupta, 2020). We performed the PCA prior to the AHP exercise to minimise this confusion. With a cumulative explained variance of 100%, six Principal Components (PCs) were extracted and the loading values of each factor were ratioed against each other to derive the relative importance of each parameter. In the first PC, with an explained variance of 28.52 % (Table 3), the Hypsometric Integral (HI) is the most important attribute with a loading value (LV) of 0.711. In the second and third PC, the most important attribute is the curvature (Cv) (LV = 0.620 and 0.681). In the fourth, fifth and sixth PCs, the most dominant attributes include the stream frequency (LV = 0.721), slope (LV = 0.510) and hypsometric integral (LV = 0.483). In ArcGIS platform these weightages were assigned to the rasters of morphometric parameters and summed to get the component-based erosion susceptibility maps. The final erosion susceptibility map (Fig. 5) of Mayurakshi river basin was then derived and is proportional to each component-based map to their explained variances. The map indicates that, by and large the basin is characterised by relatively lower erosion susceptibility. Another noteworthy observation is that the upper domain, in spite of being characterised by higher elevation, the erosion appears to be subdued. It is mentioned here that the middle domain of the Mayurakshi river basin is highly elevated with respect to relative relief, dissection index, and hypsometric integral as well as slope. The river flows through an undulating surface and cuts across a series of low-lying ranges near Massanjore and has carved out a gorge with bedrock exposures. Consequently, the middle domain of this study area is characterised by high erosion susceptibility. Downstream of Massanjore (lower domain), this river flow across a flat, featureless plain exposing alluvium.

RUSLE model

Rainfall Erosivity Factor (R)

Equation 9 has been used to ascertain the spatial variation of R Factor (Fig. 6a). As obvious, monthly rainfall as well as the annual rainfall data were required for calculating this equation. It has been stated earlier that the Tyndall Climatic Archive was used to get all the required rainfall data (Mitchell *et al.,* 2002).

For classifying the area into five natural classes, the Natural Breaks Method postulated by Jenks (1967) was applied. The average R Factor is 181.22 Mj mm $h^{-1}ha^{-1}year^{-1}$ and the range is from 174.868 Mj mm $h^{-1}ha^{-1}year^{-11}$ to 189.00 Mj mm $h^{-1}ha^{-1}year^{-1}$. By and large, the middle domain of this basin is characterised by lower values of R factor.

Soil Erodibility Factor (K)

The soil erodibility factor (K) is usually

dependent on the pedologic characteristics of the catchment. Equation 10 has been used to obtain the K Factor (Fig. 6b). It is evident that, the range of the K Factor is from 0.21 to 0.32 Mg ha h $ha^{-1}MJ^{-1}mm^{-1}$. At the northeast part of the basin, near source of the Mayurakshi river, the highest values of K Factor are obtained. This indicates that the soils are

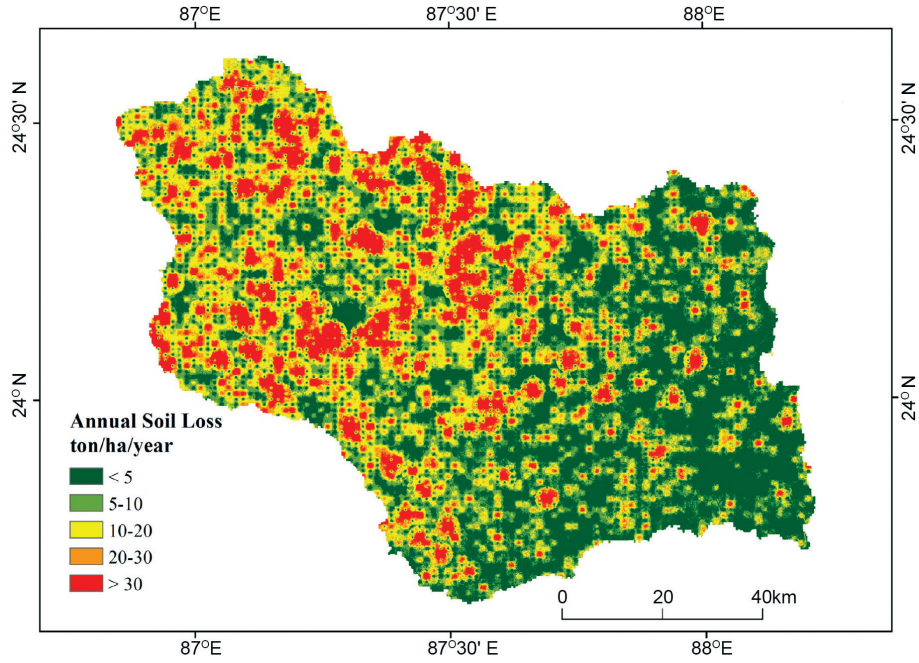

Figure 7. Spatial variation in the RUSLE-derived annual soil loss of Mayurakshi river basin.

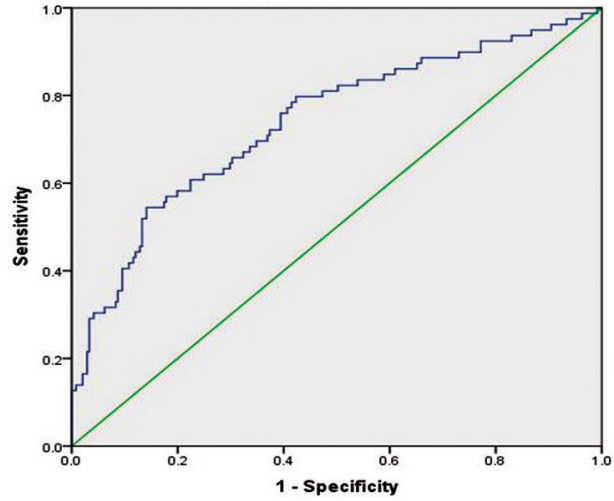

Figure 8. Validity of the two models (Morphometry and RUSLE) by the ROC Curve

highly vulnerable to erosion in these regions because here the stability and infiltration rate is low, which imply high runoff and soil loss. The K Factor value is reasonably low (0.21 to 0.24 Mg ha h $ha^{-1}MJ^{-1}mm^{-1}$) in the middle domain. Therefore, it is evident that the middle domain of this study area is characterised by high infiltration rate and low surface runoff.

Slope Length and Steepness Factor (LS)

In the exercise of soil loss prediction, the LS Factor has a direct effect. This factor affects the channelisation and direction of surface runoff. The spatial variation of the LS Factor across the studied basin has been estimated from the flow accumulation raster and the slope in radians by applying Eq.11. The mean value of LS Factor is 1.56 and ranges between <2 to >15 in Mayurakshi river basin (Fig.6c).

The LS Factor gets augmented to a considerable extent (>15) and is concentrated in the middle and scattered and isolated values of high LS Factor are observed in the upper domain. By and large, lower values of LS Factor are obtained for the maximum part of this basin. This is understandable considering the fact that a major part of the basin is flowing through a flat topography.

Crop Management Factor (C)

The ratio between the vegetation cover (NDVI) and the bare soil (NBIL) was computed to estimate the C Factor. The map (Fig. 6d) clearly shows that the value of C Factor increases downstream. The range of C Factor is between 0.46 to 1.00. The maximum value is observed in the lower domain (southeast corner) of this basin and the middle domain encounters lower values (0.0003 to 0.2163) corresponding with the areas of high slope. It can be observed in Figure 5c that the LS Factor is highest in the middle domain of the studied basin. Also, in Figure 5 it was seen that the middle domain is characterised by elevated values of the morphometric parameters and high erosion susceptibility. However, the lower values of the C Factor imply that this domain is reasonably well covered with vegetation. This gives us the importance of the land use landcover and crop management practices in the study of erosion. It is evident that in spite of the fact that the relief and slope in the middle domain is higher promoting greater erosion, but the lower C Factor, an outcome of vegetation cover helps in inhibiting the erosion or the total soil loss.

Support Practice factor (P)

It has been well recognised that areas of better land management are associated with lower magnitudes of the P Factor and hence lower amount of erosion and vice versa. Estimated P Factor is based on land use-land cover (LULC). This value has been extracted from supervised classification of LANDSAT image (Thomas *et al.,* 2018; Kolli, 2021). The entire LULC for the studied region was divided into six major categories viz., water body, dense vegetation, light vegetation, settlement, fallow land and agricultural land. The spatial variation in the magnitudes of the P Factor has been displayed in Figure 6e, A glimpse of the map reveals that a large proportion of land in the study area is covered by agricultural lands. In the upper and middle domains, there is a greater dominance of barren or fallow lands. According to the USDA P Factor Table (Table 4), the P Factor for agricultural lands is the lowest (0.5). Therefore, it may be assumed that the effectiveness of the conservation practices

factor is more pronounced in the lower reaches of the basin.

Estimating the annual soil loss (RUSLE Equation)

The sub aerial process of water-induced erosion is a complex interaction of a number of processes and causal factors, operating in a complex relationship. These factors comprise topography, climate, geology, soil, vegetation, land use and anthropogenic factors (Atoma *et al.,* 2020). In the Mayurakshi river basin, the annual soil loss was predicted by incorporating the Revised Universal Soil Loss Equation (RUSLE). The rasters of all such causal factors were undergone the Multiplication routine in the Raster Calculator Module of ArcGIS in order to get the raster of RUSLE (as per Eq. 8), depicting the spatial variation of the annual soil loss in the Mayurakshi drainage basin (Fig. 7). The estimated soil loss ranges from <5 to >30 tonsha^{-1} year^{-1} with an average soil loss of 14.20 tonsha^{-1} year^{-1}. The output soil erosion map has been divided into 5 classes: very low (<5 tonsha^{-1} year^{-1}), low (5–10 tonsha^{-1} year^{-1}), moderate (10–20 tonsha^{-1} year^{-1}), high (20–30 tonsha^{-1} year^{-1}) and very high (>30 tons ha−1 year^{-1}). This was achieved through the value distribution analysis. Even a cursory examination of Figure 7 reveals that about 22.63% of the area has been categorised as very low soil loss zone with an annual soil loss being <5 tonsha^{-1} year^{-1}. On the other hand, it is apparent that about 12.53% of the area in the Mayurakshi basin experiences annual soil losses greater than >30 tons ha−1 year−1. This is reasonably high and sustainable land management is urgently needed in this region. The other soil loss categories such as low (31.33%), moderate (23.42 %) and high (9.5%) are also observed in the study region (Table 5).

Table 5: Percentage of area in the various soil loss categories in the Mayurakshi river system.

Soil loss in tons ha^{-1} year^{-1}	Erosion classes	Area in %
<5	Very Low	23.663
5–10	Low	31.330
10–20	Moderate	23.248
20–30	High	9.543
>30	Very High	12.535

Validating morphometry-based erosion susceptibility with RUSLE-based total soil loss

For testing the reliability of the two models, selected points (randomly spaced and equidistant) were taken in the Mayurakshi river system. Special care was taken to ensure that the points are uniformly distributed across the basin. Then, the Fuzzy-AHP-based erosion susceptibility values and the RUSLE-based soil loss values were extracted for the two models. These values were then plotted in the SPSS software to get the ROC Curve (Fig. 8). A close look at Figure 8 helps in understanding the validity of the morphometry-based erosion susceptibility with RUSLE. The Area Under the Curve (AUC) is about 0.739. This implies that the reliability of the two models is about 73.90%, which is reasonably acceptable. Here, the Sensitivity (Sn) is 51.00% and Specificity (Sp) is 78.60%, which means that Sp> Sn. Sp refers to the True Positive Rate (TPR) i.e. the percentage of positives which are true and Sn refers to the True Negative Rate (TNR) i.e. the percentage of true negatives (areas of lower erosion depicted correctly). Since Sn is greater than Sp, this indicates that the areas of lower erosion are depicted correctly as compared to the areas of higher erosion.

Discussion

The term ‘hotspot’ is often used in the field of ecology which represent areas with outstanding biodiversity or a high

concentration of biological values. The broad expansion of the term hotspot in the field of hazard studies, especially erosion, is a reasonably recent trend (Chang and Bayes, 2013; Nouvas and Thomas, 2015; Chicas *et al.,* 2016). In simple words, erosion hotspots are referred to those patches/areas in a larger areal unit where the erosion undergone is significantly higher than other regions. Although there are no significant scales for identifying an area as an erosion hotspot, the statistical analysis of the erosion results may help in detection of the erosion hotspots in a region. For the detection of erosion hotspots, we have applied the Z-Score Normalisation as per Equation 13.

$$Ezi = \frac{e_i - e_i}{e_i \sigma} \qquad \text{Eq. 13}$$

where, Ezi = Z-Score Normalisation of the erosion magnitudes of pixel, = Erosion value of pixel i (as per the Fuzzy AHP based morphometry and the RUSLE based soil loss of 2018), = Average value of Fuzzy AHP based morphometry and the RUSLE based soil loss for the studied river basin and =

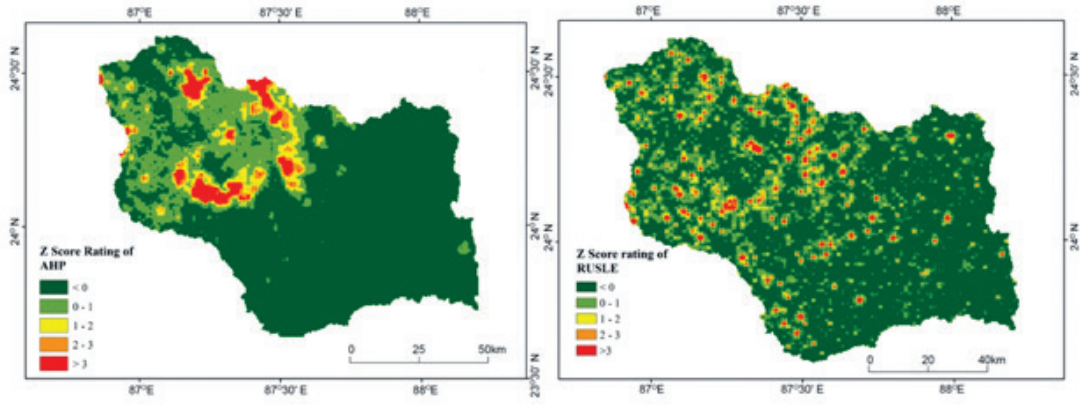

Figure 9. Z-Score Normalisation of erosion susceptibility based on: a) morphometry and fuzzy AHP and b) RUSLE model analysis for the Mayurakshi river basin.

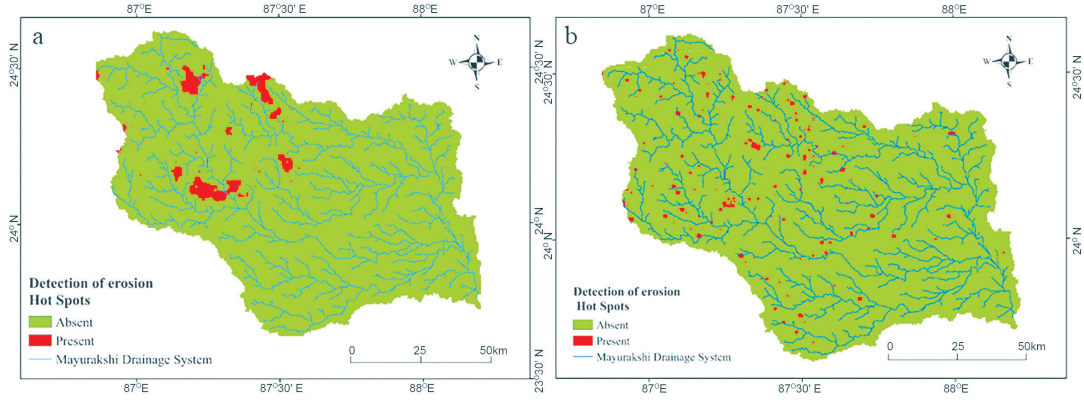

Figure 10. Erosion hotspots in the Mayurakshi river basin: a) morphometry-based and b) RUSLE model-based.

Standard Deviation of the Fuzzy AHP based morphometry and the RUSLE based soil loss for the studied basin system.

The Z-Score Normalisation maps of erosion susceptibility and soil loss by RUSLE are displayed in Figures 9a and 9b. Z Score ratings greater than 0 represent the areas where the erosion is more than average and the Z-Scores less than 0 represent regions where the erosion incurred is less than the average.

The Ezi values of each pixel in the morphometry-based erosion susceptibility and the RUSLE-based (2018) soil loss for the Mayurakshi Drainage System were then analysed and as per the Normal Probability Distribution Rule, Ezi values >3 were identified as erosion hotspots. It is a well-established fact that in case of a normal distribution, more than 99% of all observations lie between mean and three times of the standard deviation (Mean + 3 SD). Therefore, any observation with value of Z greater than +3 is regarded as an outlier. Thus, any pixel (area) with Ezi >3 will be an outlier and an erosion hotspot (Fig. 9a and 9b).

Figure 10a reveals that the erosion hotspots obtained after Z-Score Normalisation of the morphometry-based erosion potential are well pronounced. This is particularly observed in the middle domain of the Mayurakshi river system, in the vicinity of the Massanjore dam. Similarly, the upper reach of the Dwarka river displays a well-pronounced zone of erosion hotpot. A major portion of the erosion hotspots are observed in the upper basin. In all other regions (which comprise about 90% of the area), the erosion hotspots are absent. This implies that erosion is low. In the lower basin, no erosion hotspot was detected. However, the essential limitation of morphometry-based erosion susceptibility is that the anthropogenic and the pedologic parameters after often ignored. The RUSLE-based erosion hotspots are spatially mapped and displayed in Figure 9b. Even a cursory examination of Figure 10b reveals that the erosion hotspots are not as pronounced as in Figure 10a i.e., the morphometry-based erosion hotspots. Rather, they are scattered in isolated patches, the concentration of the patches being more in the middle domain of the Mayurakshi basin and the upper reach of the Dwarka river. In the lower domain, a significant aerial extent of RUSLE-based hotspots is detected. In spite of the fact that the relief and slope are not very high, the erosion and the associated soil loss is augmented by the pedologic and the vegetation cover factor. The lower domain of this basin was found to have high C Factor as seen in Figure 6d. Therefore, proper afforestation techniques can be implemented at these hotspots to check the menace of soil erosion, especially in the lower domain of the basin.

Conclusion

This study has been carried out to estimate the erosion susceptibility of the Mayurakshi basin in eastern India and to correlate and validate it with the total annual soil loss. The middle domain of this basin is displaying highest erosion susceptibility and among all the factors, slope appears to be the most dominant. It is pertinent to mention that in the middle domain, the river takes an incised course wherein a gorge has been carved out in the erosion resistant rocks which are regarded to be offshoots of the Chhotanagpur plateau (Roy *et al.,* 2022). The results of RUSLE-based annual soil loss display no major deviation from the morphometry-based erosion susceptibility wherein elevated values of soil loss are observed in the middle domain. This is further corroborated by a ROC Curve-derived validation percentage of 73.90 which

is reasonably satisfactory. However, the low sensitivity of 51% implies that areas of high erosion are not matching much. Therefore, we have considered the Z-Score normalisation for detecting erosion hotspots. This was done for both morphometry as well as RUSLE. It is observed that the RUSLE-based erosion hotspots are not only concentrated in the middle domain of the Mayurakshi basin but they are also concentrated in the upper reach of the Dwarka river. This is significant because with the addition of pedologic and anthropogenic factors to the terrain characteristics, the hotspot occurrence increases. Therefore, based on the erosion hotspots deduced by RUSLE, proper and significant soil conservation planning practices need to be introduced.

Declaration of competing interest

The authors declare that they have no known competing financial interests or personal relationships that could have appeared to influence the work reported in this paper.

References

Abdul Rahaman, S., Abdul Ajeez, S., Aruchamy, S. and Jegankumar, R. (2015) Prioritization of sub watershed based on morphometric characteristics using Fuzzy Analytical Hierarchy Process and Geographical Information System — A study of Kallar watershed, Tamil Nadu. *Aquatic Procedia*, 4: 1322–1330.

Angillieri, M.Y.E. (2008) Morphometric analysis of Colanguil river basin and flash flood hazard, San Juan, Argentina. *Environmental Geology*, 55: 107–111.

Arabameri, A., Pradhan, B., Pourghasemi, HR. and Rezaei, K. (2018) Identification of erosion-prone areas using different multi-criteria decision-making techniques and GIS. Geomatics. *Natural Hazards and Risk*, 9 (1): 1129–1155. https://doi.org/10.1080/19475705.2018.1513084.

Arnoldus, H.M.J. (1980) An Approximation of Rainfall Factor in the Universal Soil Loss Equation, In: De Boodt M., Gabriels D. (Eds.) *Assessment of Erosion*, John Wiley & Sons, Chichester: 127–132.

Asfaw, D. and Workineh, G. (2019) Quantitative analysis of morphometry on Ribb and Gumara watersheds: Implications for soil and water conservation, *International Soil and Water Conservation Research*, 7: 150–157. https://doi.org/ 10.1016/ j.iswcr.2019.02.003.

Atoma, H., Surtabhagavan, K.V. and Balakrishan, M. (2020) Soil erosion assessment using RUSLE model and GIS in Huluka watershed, Central Ethiopia. *Sustainable Water Resource Management*, 6: 2020 (1).

Bezinska, G.V. and Stoyanov, K.S. (2019) Modelling and hydro-morphometric analysis of sub-watershed: A case-study of Mesta river Southwestern Bulgaria. *European Journal of Geography*, 10(2): 77–88.

Bhat, M.S., Alam, A., Ahmad, S., Farooq, H. and Ahmad, B. (2019) Flood hazard assessment of upper Jhelum basin using morphometric parameters. *Environmental Earth Sciences*, 78: 54–71. https://doi.org/10.1007/s12665-019-8046-1.

Blanco-Canqui, H. and Lal, R. (2008) *Principles of soil conservation and management*. Springer, Netherlands: 107p.

Boender, C.G.E., de Granne, J.G. and Lootsma, F.A. (1989) Multi-criteria decision analysis with fuzzy pairwise comparisons. *Fuzzy Sets and Systems*, 29: 133–143. https://doi.org/10.1016/0165-0114(89)90187-5.

Butt, M.J., Waqas, A. and Mahmood, R. (2010) The combined effect of vegetation and soil erosion in the water resource management. *Water Resources Management*, 24(13): 3701–3714.

Chang, T.J. and Bayes, T.D. (2013) Development of erosion hotspots for a watershed. *Journal*

of Irrigation and Drainage Engineering, 139: 1011–1017.

Chicas, S.D., Omine, K. and Ford, J.B. (2016) Identifying erosion hotspots and assessing communities' perspectives on the drivers, underlying causes and impacts of soil erosion in Toledo's Rio Grande Watershed: Belize. *Applied Geography*, 68, 57–67.

Civeira, M.S., Ramos, C.G., Oliveira, M.L.S., Kautzmann, R.M., Taffarel, S.R., Teixeira, E.C. and Silva, L.F. (2016a) Nano-mineralogy of suspended sediment during the beginning of coal rejects spill. *Chemosphere*,145,142–147.

Civeira, M.S., Oliveira, M., Hower, J., Agudelo-Castañeda, D., Taffarel, S.R., Ramos, C., Kautzmann, R.M. and Silva, L.F. (2016b) Modification, adsorption, and geochemistry processes on altered minerals and amorphous phases on the nanometer scale: examples from copper mining refuse, Touro, Spain. *Environmental Science and Pollution Research*, 23: 6535–6545.

Daoud, J.I. (2012) Multicollinearity and regression analysis. *Journal of Physics: Conference Series 949*, 012009. https://doi.org/10.1088/1742-6596/949/1/012009.

Dar, I.A., Prabu, P. and Das, M.A. (2013) Erosion Modeling in Hard Rock Terrain Using Morphometry: A Case Study from Tamil Nadu, India. *Environmental Quality Management*, 23 (2): 47–60. https://doi.org/10.1002/tqem.21360.

Das, A., Agrawal, R. and Mohan, S. (2015) Topographic correction of ALOS-PALSAR images using InSAR-derived DEM. *Geocarto International*, 30(2): 145–153. https:// doi.org/10.1080/ 10106049.2014.883436.

Das, B., Bordoloi, R., Thungon, L.T., Paul, A., Pandey, P.K., Mishra, M. and Tripathi, O.P. (2020) An integrated approach of GIS, RUSLE and AHP to model soil erosion in West Kameng Watershed, Arunachal Pradesh. *Journal of Earth System Science*, 129(94). https://doi.org/10.1007/s12040-020-1356-6.

Das, B., Paul, A., Bordoloi, R., Tripathi, O.P. and Pandey, P.K. (2018) Soil erosion risk assessment of hilly terrain through integrated approach of RUSLE and geospatial technology: A case study of Tirap District, Arunachal Pradesh. *Modelling Earth Systems and Environment*, 4 (1): 373–381.

David, W.P. (1988) *Soil and Water Conservation Planning: Policy Issues and Recommendations*. J. Philipp. Dev., 15: 47–84.

Dormann, C.F., Elith, J., Bacher, S., Buchmann, C., Carl, G., Carre, G., Garcia, Marquez, J.R., Gruber, B., Lafourcade, B., Leitao, P.J., Munkemuller, T., McLean, C., Osborne, P.E., Reineking, B., Schroder, B., Skidmore, A.K., Zurrell, D. and Lautenbach, S. (2013). Collinearity: a review of methods to deal with it and a simulation study evaluating their performance. *Ecography*, 36: 27–46. http://doi.org/10.1111/j.1600-0587.2012.07348.

Dutta, M., Saikia, J., Taffarel, S.R., Waanders, F.B., Medeiros, D., Cutruneo, C.M. and Saikia, B.K. (2017) Environmental Assessment and nano-mineralogical characterization of coal, overburden, and sediment from Indian coal mining acid drainage. *Geoscience Fronter*, 8: 1285–1297.

Evans, I. S. (1980) An integrated system of terrain analysis and slope mapping. *Zeitschrift Fur Geomorphologie,* 36: 274–295.

Evans, I.S. (2012) Geomorphometry and landform mapping: What is a landform? *Geomorphology*, 137 (1): 94–106.https://doi.org/10.1016/j.geomorph.2010.09.029.

Farhan, A.Y., Zregat, D. and Farhan, I. (2013) Spatial estimation of soil erosion risk using RUSLE approach, RS, and GIS techniques: a case study of Kufranja Watershed Northern Jordan. *Journal of Water Resource and Protection*, 5:1247–1261.

Gebremicael, T.G., Mohamed, Y.A., Betrie, G.D., Zaag, P. and Teferi, E. (2013) Trend analysis of runoff and sediment fluxes in the Upper Blue Nile basin: a combined analysis of statistical tests, physically based models and land-use

maps. *Journal of Hydrology*, 482: 57–68.

Goudie, A.S. (2004) *Encyclopedia of Geomorphology*, Routledge, London: 1156p.

Gregory, K.J. (1999) Drainage basins. In: Environmental Geology. *Encyclopedia of Earth Science*. Springer, Dordrecht. https://doi.org/10.1007/1-4020-4494-1_83.

Griffin, M.L., Beasley, D.B., Fletcher, J.J. and Foster, G.R. (1988) Estimating soil loss on the topographically non-uniform field and farm units. *Soil Water Conservation*, 43: 326–331.

Haidara, I., Tahri, M., Maanan, M. and Hakdaoui, M. (2019) Efficiency of Fuzzy Analytic Hierarchy Process to detect soil erosion vulnerability. *Geoderma*, 354(11): 35–83. https://doi.org/10.1016/j.geoderma.2019.07.011.

Haile, G.W. and Fetene, M. (2012) Assessment of soil erosion hazard in Kilie catchment, East Shoa, Ethiopia. *Land Degradation and Development*, 23 (3): 293–306.

Hair, J.F. Jr., Anderson, R.E., Tatham, R. L. .and Black, W.C. (1995) *Multivariate data analysis* (3rd Edition), Macmillan, USA: 816p.

Horton, R.E. (1932) Drainage basin characteristics. *Transactions American Geophysical Union*, 13: 350–361. https://doi.org/10.1029/TR013i001p00350.

Horton, R.E. (1945) Erosional development of streams and their drainage basins: Hydrophysical approach to quantitative morphology. *Bulletin of the Geological Society of America*, 56(3): 275−370.

Islam, A. and Deb, Barman, S. (2020) Drainage basin morphometry and evaluating its role on flood-inducing capacity of tributary basins of Mayurakshi river, India. *SN Applied Sciences*, 2: 1087.

Jenks, G. F. (1967) The data model concept in statistical mapping. *International Yearbook of Cartography*, 07: 186–190.

Kachouri, S., Achour, H., Abida, H. and Bouaziz, S. (2014) Soil erosion hazard mapping using Analytic Hierarchy Process and logistic regression: a case study of Haffouz watershed, central Tunisia. *Arabian Journal of Geosciences*, 8: 4257–4268. https:// doi.org/10.1007/s12517-014-1464-1.

Kadam, A.K., Jaweed, T.H., Kale, S.S., Umrikar, B.N. and Sankhua, R.N. (2019) Identification of erosion-prone areas using modified morphometric prioritization method and sediment production rate: A remote sensing and GIS approach. Geomatics. *Natural Hazard and Risk*, 10(1): 986–1006. https:// doi.org/10.1080/ 19475705.2018.1555189.

Kale, V.S., Sengupta, S., Achyuthan, H. and Jaiswal, M.K. (2014) Tectonic controls upon Kaveri River drainage, cratonic Peninsular India: Inferences from longitudinal profiles, morphotectonic indices, hanging valleys and fluvial records. *Geomorphology*, 227: 153–165.

Keat, P.G., Young, P.K.Y. and Banerjee, S. (2009) *Managerial Economics*, 6th Edition, Pearson Education Inc: 626p.

Kim, J., Choi, J., Choi, C. and Park, S. (2013) Impacts of changes in climate and land use land cover under IPCC RCP scenarios on streamflow in the Hoeya River Basin, Korea. *Science of the Total Environment*: 452–453.

Kim, J.B., Saunders, P. and Finn, J.T. (2005) Rapid Assessment of soil erosion in the Rio Lempa Basin, Central America, using the Universal Soil Loss Equation and Geographic Information Systems. *Environmental Management*, 36: 872–885.

Kolli, M.K., Opp, C. and Groll, M. (2021) Estimation of soil erosion and sediment yield concentration across the Kolleru Lake catchment using GIS. *Environmental Earth Sciences*, 80: 161.

Kuhni, A, and Pfiffner, O.A. (2001) The relief of the Swiss Alps and adjacent areas and its relation to lithology and structure: topographic analysis from a 250-m DEM. *Geomorphology*, 41(4): 285–307.

Kumar, S. and Gupta, S. (2016) Geospatial

approach in mapping soil erodibility using CartoDEM–A case study in hilly watershed of Lower Himalayan Range. *Journal of Earth System Science*, 125 (7): 1463–1472. http://doi.org/10.1007/s12040-016-0738-2.

Lee, J.H. and Heo, J.H. (2011) Evaluation of estimation methods for rainfall erosivity based on annual precipitation in Korea. *Journal of Hydrology*, 409: 30–48, https://doi.org/10.1016 /j.jhydrol.2011.07.031.

Lee, S. (2004) Soil erosion assessment and its verification using the Universal Soil Loss Equation and Geographic Information System: A case study at Boun, Korea. *Environmental Geology*. 45: 457–465.

Lim, K.J., MyungSagong, M., Engel, B.A., Tang, Z., Choi, J. and Kim, K.M. (2005) GIS-based sediment assessment tool. *Catena*, 64: 61–80.

Luo, X. and Dimitrakopoulos, R. (2003) Data-driven fuzzy analysis in quantitative mineral resource assessment. *Computers& Geosciences*, 29(1): 3–13. http:// doi.org/10.1016/ S0098-3004(02)00078-X.

Magner, J.A. and Brooks, K.N. (2008) Predicting stream channel erosion in the lacustrine core of the upper Nemadji River, Minnesota (USA) using stream geomorphology metrics. *Environmental Geology*, 54: 1423–1434. https://doi.org/10.1007/s00254-007-0923-3.

Mather, P.M. and Doornkamp, J.C. (1970) Multivariate analysis in geography with particular reference to drainage-basin morphometry. *Transactions of the Institute of British Geographers*, 51: 163–187. http://doi.org/10.2307/621768.

McCool, D.K., Foster, G.R., Mutchler, C.K. and Meyer, L. D. (1989) Revised slope length factor for the Universal Soil Loss Equation. *Transactions of the ASAE*, 32: 1571–1576.

Mela, C.F.and Kopalle, P.K. (2002) The impact of collinearity on regression analysis: the asymmetric effect of negative and positive correlation. Journal of Applied Economics, 34(6): 667–677. https://doi.org/10.1080/00036840110058482.

Melton, M.A. (1965) The geomorphic and paleoclimatic significance of alluvial deposits in Southern Arizona. *Geological Society of America Bulletin*, 73(1): 1–38. https:// doi.org/10.1086/627044.

Mesa, L.M. (2006) Morphometric analysis of a subtropical Andean basin (Tucuman, Argentina). *Environmental Geology*, 50(8): 1235–1242. https:// doi.org/10.1007/ s00254-006-0297-y.

Meshram, S.G. and Sharma, S.K. (2017) Prioritization of watershed through morphometric parameters: A PCA-based approach. *Applied Water Science*, 7: 1505–1519. https://doi.org/10.1007/s13201-015-0332-9.

Mistri, P. and Sengupta, S. (2020) Multi Criteria Decision Making Approach to Agricultural Land Suitability classification of Malda District of Eastern India. *Natural Resources Research*, 29: 2237–2256. https://doi.org/10.1007/s11053-019-09556-8.

Mitchell, T.D., Hulme, M. and New, M. (2002) Climate data for political areas. *Area*, 34: 109–112.

Moore, I.D. and Burch, G.J. (1986a) Modeling erosion and deposition. Topographic effects. *Transactions of American Society of Agriculture Engineering*, 29: 1624–1630. https://doi.org/10.13031/2013.30363.

Moore, I.D. and Burch, G.J. (1986b) Physical Basis of the Length Slope Factor in the Universal Soil Loss Equation. *Soil Science Society of America*, 50: 1294-1298. http://dx.doi.org/10.2136/sssaj1986.03615995005000050042x.

Moore, I.D. and Wilson, J.P. (1992) Length-slope factors for the revised universal soil loss equation: simplified method of estimation. *Soil Water Conservation*, 47: 423–428.

Moore, I.D., Grayson, R.B. and Ladson, A.R. (1991) Digital terrain modelling: A review of hydrological, geomorphological and biological applications. *Hydrological*

Processes, 5(1): 3–30. https://doi.org/10.1002/hyp.3360050103.

Mela, C.F. and Kopalle, P.K. (2002) The impact of collinearity on regression analysis: the asymmetric effect of negative and positive correlation. *Journal of Applied Economics*, 34(6): 667–677. https://doi.org/10.1080/00036840110058482.

Mutua, B.M., Klik, A. and Loiskandl, W. (2006) Modelling soil erosion and sediment yield at a catchment scale: the case of Masinga catchment, Kenya. *Land Degradation & Development*, 17(5): 557–570. http://dx.doi.org/10.1002/ldr.753.

Niipele, J.N., and Chen, J. (2019) The usefulness of ALOS-PALSAR dem data for drainage extraction in semi-arid environments in the Iishana subbasin. Journal of Hydrology: Regional Studies, 21: 57–67. https://doi.org/10.1016/j.ejrh.2018.11.003.

Nir, D. (1957) The ratio of relative and absolute altitudes of Mt. Carmel: A contribution to the problem of relief analysis and relief classification. Geographical Review, 47(4): 564–569. https://doi.org/10.2307/211866.

Nouvas, V. and Thomas, K.V. (2015) Erosion hotspots along southwest coast of India. *Aquatic Procedia*, 4: 548–555.

Oliveira, M.L.S., Saikia, B.K., Da, Boit, K., Pinto, D., Tutikian, B.F. and Silva, L.F.O. (2019) River dynamics and nanoparticle formation: a comprehensive study on the nanoparticle geochemistry of suspended sediments in the Magdalena River. Caribbean Industrial Area. *Journal of Cleaner Production*, 213: 819–824.

Panagos, P., Borrelli, P., Meusburger, K., Yu, B., Klik, A., Jae Lim, K. and Ballabio, C. (2017) Global rainfall erosivity assessment based on high-temporal resolution rainfall records. *Scientific Reports,* 7 (1): 4175. https://doi.org/10.1038/s41598-017-04282-8.

Pandey, A., Mathur, A., Mishra, S.K. and Mal, B. C. (2009) Soil erosion modelling of a Himalayan Watershed using RS and GIS. *Environmental Earth Sciences*, 59: 399–410.

Pavlis, N.K., Holmes, S.A., Kenyon, S.C., and Factor, J.K. (2012) The development and evaluation of the earth gravitational model 2008 (EGM 2008). *Journal of Geophysical Research*, 117(B4): B04406. https://doi.org/10.1029/ 2011JB008916.

Pike, R.J. and Wilson, S.E. (1971) Elevation-Relief Ratio, Hypsometric Integral, and Geomorphic Area-Altitude Analysis. *GSA Bulletin*, 82(4): 1079–1084. https://doi.org/10.1130/0016-7606(1971)82[1079:ERHIAG]2.0.CO;2.

Prabhakar, A.K., Singh, K.K., Lohani, A.K. and Chandniha, S.K. (2019) Study of Champua watershed for management of resources by using morphometric analysis and satellite imagery. *Applied Water Science*, 9: 127. https://doi.org/10.1007/s13201-019-1003-z.

Rawat, K.S. and Mishra, A.K. (2016) Evaluation of relief aspects morphometric parameters derived from different sources of DEMs and its effects over time of concentration of runoff. *Earth Science Informatics*, 9: 409-424. https://doi.org/10.1007/s12145-016-0261-7.

Renard, K.G. and Foster, G.R. (1983) Soil conservation: principles of erosion by water. In: Dregne HE, Willis WO (eds) *Dryland agriculture. Agronomy Monograph,* No. 23.

Renard, K.G. and Freimund, J.R. (1994) Using monthly precipitation data to estimate the R factor in the revised USLE. *Journal of Hydrology*, 157: 287–306.

Renard, K.G., Foster, G.R., Weesies, G.A., McCool, D. K., and Yoder, D.C. (1997) Predicting soil erosion by water: a guide to conservation planning with the revised universal soil loss equation (RUSLE). *Agriculture Handbook No. 703*, USDA, Washington DC: 384p.

Roy, S., Das, S., and Sengupta, S. (2023) Predicting terrain erosion susceptibility from drainage basin morphometry using ALOS-PALSAR DEM: Analysis from PCA-weighted AHP approach in a river system of Eastern India. *Environment, Development and*

Sustainability, 25: 9589–9617. https://doi.org/10.1007/s10668-022-02450-z.

Saaty, T.L. (1980) *The analytic hierarchy process: Planning, priority setting, resource allocation*. New York, NY: McGraw Hill International: 287p.

Sarkar, A., Roy, L., Das, S., and Sengupta, S. (2021) Fluvial response to active tectonics: analysis of DEM-derived longitudinal profiles in the Rangit River Basin, Eastern Himalayas, India. *Environmental Earth Sciences*: 258. https:// doi.org/ 10.1007/ s12665-021-09561-2.

Schumm, S.A. (1956) The evolution of drainage systems and slopes inbadlands at Perth Amboy, New Jersey. *Geological Society of America Bulletin*, 67(5): 597–646. https://doi.org/10.1130/0016-7606 (1956)67[597:EODSAS]2.0.CO;2.

Setegn, S.G., Dargahi, B., Srinivasan, R. and Melesse, A.M. (2010) Modeling of sediment yield from Anjeni-Gauged Watershed, Ethiopia using SWAT model. *Journal of African Water Resource Association*, 46: 514–526.

Sheikh, A.H., Palria, S. and Alam, A. (2011) Integration of GIS and Universal Soil Los Equation (USLE) for soil loss estimation in a Himalayan Watershed. *Recent Research in Science and Technology*, 3: 51–57.

Singh, O., Sarangi, A. and Sharma, M.C. (2008) Hypsometric Integral estimation methods and its relevance on erosion status of north-western Lesser Himalayan watersheds. *Water Resources Management*, 22: 1545–1560. http://doi.org/10.1007/s11269-008-9242-z.

Singh, O., Sarangi, A. and Sharma, M.C. (2008) Hypsometric Integral estimation methods and its relevance on erosion status of north-western Lesser Himalayan watersheds. *Water Resources Management*, 22: 1545–1560. http://doi.org/10.1007/s11269-008-9242-z.

Sreedevi, P.D., Sreekanth, P.D., Khan, H.H. and Ahmed, S. (2013) Drainage morphometry and its influence on hydrology in a semi-arid region: Using SRTM data and GIS. *Environmental Earth Sciences*, 70: 839–848. http://doi.org/10.1007/s12665-012-2172-3.

Strahler, A.N. (1956). Quantitative Slope Analysis. *Geological Society of America Bulletin*, 67: 571–596. https://doi.org/10.1130/0016-7606(1956)67.

Strahler, A.N. (1957) Quantitative analysis of watershed geomorphology. *Transactions American Geophysical Union*, 38: 913-920. https:// doi.org/ 10.1029/TR038i006p00913.

Thomas, J., Joseph, S. and Thrivikramji, K.P. (2018) Assessment of soil erosion in a tropical mountain river basin of the southern western ghat, India using RUSLE and GIS. *Geoscience Frontiers*: 9, 893–906.

Vommi, V.B. (2017) TOPSIS with statistical distances: A new approach to MADM. *Decision Science Letters*, 6(1): 49-66.

Wallis, J.R. (1965) Multivariate statistical methods in hydrology—A comparison using data of known functional relationship. *Water Resources Research*, 4: 447 https://doi.org/10.1029/WR001i004p00447.

Wang, H., Wang, G., Wang, F., Sassa, K. and Chen, Y. (2008) Probabilistic modelling of seismically triggered landslides using Monte Carlo simulations. *Landslides*, 5: 387–395. https://doi.org/10.1007/s10346-008-0131-6.

Wischmeier, W.H. and Smith, D.D. (1978) Predicting rainfall erosion losses: a guide to conservation planning. *Agriculture Handbook No. 537*, USDA, Washington, DC: 58p.

Date received: 15 March 2025
Date accepted after revision: 24 July 2025